Original Article

Check for updates

Available online at
www.heca-analitika.com/ljes

Leuser Journal of Environmental Studies

Vol. 3, No. 2, 2025

Optimizing Palm Oil Biodiesel Purity for a Cleaner Environment: Urea Complexation and RSM Approach

Zohera Zohera [1,2,*], Zuchra Helwani [1] and Sunarno Sunarno [1]

[1] Department of Chemical Engineering, Universitas Riau, Pekanbaru 28293, Indonesia; zohera1784@grad.unri.ac.id (Z.Z); zuchra.helwani@lecturer.unri.ac.id (Z.H); sunarno@lecturer.unri.ac.id (S.S)
[2] PT. Rekayasa Engineering, Pekanbaru 28263, Indonesia

* Correspondence: zoherazohera@gmail.com

Article History

Received 17 May 2025
Revised 13 July 2025
Accepted 22 July 2025
Available Online 27 July 2025

Keywords:
Biodiesel fractionation
UIC
UCF
NUCF
Response Surface Methodology
Iodine value

Abstract

The performance and stability of biodiesel are strongly influenced by its fatty acid composition, particularly the balance between saturated (SFA) and unsaturated fatty acids (UFA). This study employed the urea inclusion compound (UIC) method to fractionate biodiesel and optimize conditions for obtaining a high-yield, high-quality saturated fraction (UCF). A central composite design (CCD) under response surface methodology (RSM) was used to evaluate the effects of urea-to-methanol ratio, crystallization temperature, and crystallization time on UCF and NUCF yields and iodine values. Experiments were conducted using a range of crystallization temperatures (18–22°C), times (3–5 h), and urea-to-methanol ratios (1:1.5–1:2.5). The response variables were analyzed and optimized using desirability functions. The results showed that all three factors significantly influenced both the yield and iodine value of the fractions. The optimal condition, urea-to-methanol ratio of 1:1.73, temperature of 19.99°C, and time of 5 h, yielded 81.59% UCF with an iodine value of 36.65 g I_2/100 g, falling within the desired range for high-performance saturated biodiesel. In contrast, the NUCF fraction was minimized to 1.76% and enriched in PUFA. These findings demonstrate the potential of UIC-based fractionation for producing biodiesel with improved oxidative stability and combustion properties, aligning with international quality standards and contributing to more sustainable fuel formulations.

1. Introduction

The global energy crisis and the escalating urgency to mitigate climate change have compelled nations to shift towards more sustainable energy systems. Among various renewable energy options, biodiesel has gained significant attention due to its potential to reduce greenhouse gas (GHG) emissions, biodegradability, and compatibility with existing diesel infrastructure [1–3]. As a clean-burning fuel derived from biological sources such as vegetable oils or animal fats, biodiesel plays an increasingly vital role in achieving environmental and energy security goals. In Indonesia, biodiesel serves not only as a strategy to reduce fossil fuel imports but also as a pathway to enhance the economic value of crude palm oil (CPO), which is the primary feedstock for biodiesel in the country [4].

The Indonesian government's biofuel program, regulated under Presidential Regulation No. 5/2006 and further supported by MEMR Regulation No. 12/2015, has evolved rapidly from a 2.5% blending mandate (B2.5) in 2008 to B40 in 2025 [4]. This policy aligns with Indonesia's long-term commitment to achieving net-zero emissions by 2060 and demonstrates the strategic role of biodiesel in national climate action plans. However, the widespread

adoption of biodiesel still faces technical limitations, particularly poor cold-flow properties, low oxidative stability, and limited storage performance, which pose environmental and operational risks [5, 6]. These issues are closely tied to the fatty acid composition of biodiesel, especially the ratio between saturated (SFA), monounsaturated (MUFA), and polyunsaturated fatty acids (PUFA) [1, 7].

PUFAs, with multiple double bonds, are highly susceptible to oxidation, leading to the formation of peroxides and gums that degrade fuel quality and increase harmful emissions [8]. Conversely, SFAs enhance oxidative stability and increase cetane numbers but negatively affect cold-flow performance due to higher crystallization tendencies [9]. To achieve premium-quality biodiesel, defined by oxidation stability >20 h, cloud point <5°C, and cetane number >60, many researchers have explored fractionation techniques to selectively reduce PUFA while retaining desirable SFA and MUFA content [10, 11]. Urea inclusion compound (UIC) technology is one of the most promising methods, offering a simple and environmentally friendly route for fatty acid separation under mild conditions [11, 12].

UIC operates based on the ability of linear-chain SFAs to form crystalline complexes with urea, while PUFA and branched-chain FAME remain in the liquid phase. This results in two major fractions: a urea-complexed fraction (UCF), rich in stable FAMEs, and a non-urea-complexed fraction (NUCF), dominated by oxidation-prone PUFA [10, 13]. In the UIC process, urea forms hexagonal channel-like crystals through hydrogen bonding networks, which selectively entrap straight-chain saturated fatty acid methyl esters (FAMEs) via van der Waals interactions and steric compatibility [10, 12]. Unsaturated FAMEs, especially PUFA, possess one or more cis-double bonds that introduce kinks in the molecular structure, preventing them from fitting into the linear cavities of urea crystals. This selectivity is governed not only by molecular geometry but also by crystallization kinetics, solubility of components in the solvent system, and the thermodynamic driving force of inclusion under cooling conditions. Parameters such as urea-to-methanol ratio, temperature, and time directly influence the rate of complexation, mass transfer resistance, and ultimate purity of the separated fractions [9, 11, 13]. An optimized combination of these variables is thus crucial to maximizing the yield of the UCF fraction with desirable fuel properties while minimizing the environmental impact from oxidation-prone PUFA. Several studies have applied this method with various feedstocks. Jiang et al. [9] obtained 98% PUFA purity from soybean FAME; Guo et al. [14] successfully reduced iodine value to 49 from waste cooking oil; and Helwani et al. [15] reported an iodine value of 44.01 and oxidation stability of 18.6 hours from palm-based FAME at 20°C. Despite these advances, most studies investigated only one or two variables at fixed levels, such as temperature or time, without considering interactions between parameters.

Given the nonlinear and interdependent nature of variables such as urea-to-solvent ratio, crystallization temperature, and time, a more holistic optimization strategy is required. Response Surface Methodology (RSM) combined with Central Composite Design (CCD) enables the exploration of complex design spaces while minimizing experimental burden [16]. This statistical approach not only allows the identification of optimal conditions but also facilitates modeling of interaction effects among variables, something that previous one-factor-at-a-time studies have overlooked.

Therefore, this study aims to optimize the fractionation of palm-based biodiesel using the UIC method by applying RSM–CCD to three critical parameters: urea-to-methanol ratio (1:1.5–1:2.5), crystallization temperature (18–22°C), and crystallization time (3–5 h). The outcomes, fraction yield, and iodine value will be evaluated to determine the best conditions for producing high-quality biodiesel with improved oxidative stability and lower environmental risk. By reducing PUFA content effectively, this research supports the development of cleaner, more durable biofuels, in line with global efforts toward sustainable energy transitions and environmental protection. This study also targets an iodine value range of 30–40 g I_2/100 g, which has been widely recognized as optimal for achieving both high oxidation stability and low cold-flow sensitivity, making the resulting biodiesel more suitable for long-term storage and operation in tropical to sub-tropical climates [17]. By achieving this balance, the study aims to contribute both scientifically (through multivariable modeling of the UIC process) and practically (toward scalable production of cleaner biodiesel).

2. Materials and Methods

All experimental runs were performed in duplicate. Results are reported as means ± standard deviation.

2.1. Overview and Research Questions

This study investigated the fractionation of biodiesel via the Urea Inclusion Compound (UIC) method using a Response Surface Methodology (RSM) approach. The primary goal was to optimize the crystallization parameters to produce a biodiesel fraction with a targeted iodine value (IV) of 30–40 g I2/100 g, which reflects improved oxidative stability and environmental

performance. The specific research questions addressed were:

- How do the urea-to-methanol ratio, crystallization temperature, and crystallization time affect UCF and NUCF yields?
- How do these variables influence the iodine values of UCF and NUCF?
- What are the optimum conditions to maximize UCF yield and IV within the target range?

2.2. Materials and Tools

The materials used in this study included biodiesel sourced from PT. Wilmar, methanol, urea (46% N), and distilled water. For the analysis of iodine value, sodium thiosulfate pentahydrate ($Na_2S_2O_3 \cdot 5H_2O$), 0.5% starch solution, 20% potassium iodide (KI) solution, Wijs reagent, and carbon tetrachloride ($CHCl_3$) were employed. The apparatus used in the experimental procedures comprised an analytical balance, Erlenmeyer flasks, spatulas, beakers, magnetic stirrer with heater, round-bottom flask with three necks and condenser, thermometer, graduated cylinders, dropper pipettes, oven, filter paper for NUCF filtration, glass separatory funnel for isolating SFA, MUFA, and PUFA from residues, as well as volumetric flasks and burettes.

2.3. Biodiesel Fractionation Process

This research was conducted in three main stages. The first stage involved the biodiesel fractionation process, which consisted of dissolution and crystallization. In this stage, urea was dissolved in methanol at a specific ratio using a three-neck round-bottom flask equipped with a magnetic stirrer, and the solution was stirred at 500 rpm and heated at a rate of ~5°C/min to reach 60°C. After the biodiesel 40 mL addition, the mixture was stirred continuously at the same speed. The cooling to room temperature occurred passively at ambient rate (~2°C/min), followed by controlled crystallization using a refrigerated water bath to maintain target temperatures." The crystallization process was carried out at temperatures of 18°C, 20°C, and 22°C for durations of 3, 4, and 5 hours, respectively. This process resulted in the formation of crystals representing the urea complexed fraction (UCF) and a filtrate corresponding to the non-urea complexed fraction (NUCF).

2.4. Separation of UCF and NUCF

The second stage involved the separation of UCF and NUCF fractions. The separation was carried out using a Büchner funnel, where the concentrated crystal fraction (UCF) contained saturated fatty acids (SFA) and a small amount of mono-unsaturated fatty acids (MUFA). In contrast, the filtrate (NUCF) contained polyunsaturated fatty acids (PUFA). After separation, both fractions were washed with distilled water at 70°C until the wash solution became clear and the washing was deemed complete when the wash filtrate reached pH 7.0 ± 0.2, indicating the removal of residual methanol and urea The samples were then dried in an oven to remove residual water, methanol, and distilled water before further analysis. Samples were dried in an oven at 105°C until the weight was constant. The dried UCF and NUCF fractions were stored in airtight amber vials at 4°C prior to iodine value analysis, and analyzed within 72 hours to avoid oxidative degradation."

2.5. %Yield Analysis

The yield was calculated by comparing the weight of the obtained UCF or NUCF fraction with the initial weight of biodiesel, then multiplying by 100%. The yield reflects the efficiency of the separation between the complexed and non-complexed fractions (Equation 1).

$$\%Yield = \frac{Weight\ of\ UCF\ or\ NUCF\ (g)}{Initial\ biodieselw\ eight\ (g)}\ x100\% \qquad (1)$$

2.6. Iodine Value Analysis

The iodine value (IV) is used as an indicator of the degree of unsaturation in fatty acids within a sample. A higher iodine value indicates a greater number of double bonds present in the fatty acid chains. The iodine value was determined using the Wijs method, which involves the reaction between unsaturated fatty acids and an iodine solution in chloroform, followed by titration with a standard sodium thiosulfate solution. The sodium thiosulfate solution was first standardized by SNI 06-4987-1999. The iodine value was calculated based on the volume of sodium thiosulfate solution used in the titration of both the blank and the sample, the normality of the solution, and the weight of the sample, using the prescribed formula.

In this study, it was assumed that a second-order response surface model could be used to determine the optimal processing conditions. This assumption is based on the model's capability to identify a stationary point, which may represent a maximum, minimum, or saddle point in the observed response. To construct this model, the Central Composite Design (CCD) was employed, allowing for analysis of linear, quadratic, cubic, and interaction effects among process variables. The process variables investigated included the FAME-to-methanol ratio, crystallization time, and crystallization temperature, with the observed responses being the yield and iodine value of the resulting UCF and NUCF fractions. Table 1 presents the range and levels of each

Table 1. Levels of fractionation variables used in this experiment.

Variable	Coded Symbol	Unit	Levels				
			-a	**-1**	**0**	**1**	***a***
FAME/Methanol Ratio	X_1	%(w/v)	1.1591	1.5	2	2.5	2.841
Crystalization Temp	X_2	℃	16.6364	18	20	22	23.364
Crystalization Time	X_3	hr	2.31821	3	4	5	5.682

α = 1.68

independent variable used in this study. The relationship between the coded and uncoded variables is expressed in Equations 2–4.

$$X_1 = \frac{\left(\frac{FAME}{methanol\ ratio}\right) - \left(\frac{low + high}{2}\right)}{\frac{igh - low}{2}} \quad (2)$$

$$X_2 = \frac{CrytallizationTemp - \left(\frac{low + high}{2}\right)}{\frac{igh - low}{2}} \quad (3)$$

$$X_3 = \frac{CrytallizationTime - \left(\frac{low + high}{2}\right)}{\frac{igh - low}{2}} \quad (4)$$

The experimental runs were randomly ordered using the randomization function in DDX7 software to minimize systematic error. Table 1 presents the actual and coded levels used. The Central Composite Design (CCD) implemented in this study comprised twenty experimental runs, constructed from three components: eight runs from a two-level factorial design, six axial (or star) points, and six replicates at the center point. The two-level factorial portion, expressed as 2^k with k = 3 factors, covered both minimum and maximum levels, resulting in the following eight combinations: (-1, -1, -1), (-1, -1, 1), (-1, 1, -1), (-1, 1, 1), (1, -1, -1), (1, -1, 1), (1, 1, -1), and (1, 1, 1). The six axial points were positioned along each axis at the following coordinates: (−α, 0, 0), (+α, 0, 0), (0, −α, 0), (0, +α, 0), (0, 0, −α), and (0, 0, +α). The design also included six center points located at (0, 0, 0) to evaluate experimental error and ensure precision. The value of alpha (α) was set to 1.68, calculated using the formula α = (nF)^(1/4), where nF is the number of factorial points.

2.7. Statistical Validation & Model Adequacy

Outliers were identified through residual vs. predicted plots. Data points with standardized residuals >±2.5 were flagged. Normality of residuals was assessed using the Anderson-Darling test. Model adequacy was further validated via lack-of-fit test, adjusted R^2, predicted R^2, and PRESS statistics. All analyses were performed using DDX7.

3. Results and Discussion

3.1. Mechanistic Insights of UIC Fractionation

During the UIC process, urea acts as a host matrix, forming hydrogen-bonded channel-type inclusion complexes with straight-chain saturated and monounsaturated fatty acids (SFA and MUFA), driven by molecular geometry and polarity. Methanol serves as a wetting agent and solvent, facilitating urea dissolution and enhancing the diffusion of fatty acids. The crystallization phase relies on supersaturation dynamics, where solute incorporation into urea channels is controlled by mass transfer, cooling rate, and temperature-dependent solubility.

Table 2 reveals that the optimum biodiesel fractionation conditions are achieved at a crystallization temperature of 20°C, 4 hours of duration, and a urea: methanol ratio of 1:2, producing a UCF %yield of 79.06% and an iodine value of 31.58 g I2/100 g. This iodine value indicates stable biodiesel with an optimal degree of saturation, reducing double bonds and unsaturated chains that are prone to oxidation. Variations in urea concentration, temperature, and crystallization time were proven to significantly affect the efficiency of inclusion complex formation and fraction separation, making the determination of these parameters essential to obtain high-performance and chemically stable biodiesel.

3.2. Model Development and Adequacy Testing

Quadratic models were developed for four response variables: UCF yield, NUCF yield, IV UCF, and IV NUCF. The adequacy of these models was confirmed by ANOVA (Table 3), showing significant model terms ($p < 0.05$) and acceptable Lack of Fit ($p > 0.05$). The model for IV NUCF presented a lower R^2 (0.64), suggesting a moderate fit. This may be attributed to the limited sensitivity of IV NUCF to the tested variables or external experimental variability (e.g., fatty acid distribution in NUCF phase).

3.3. Effect of Process Variables on UCF Yield

Among the studied factors, the urea-to-methanol ratio had the strongest influence on UCF yield (Equation 5),

Table 2. %Yield and iodine value results of fractionation.

No	Urea : Methanol Ratio (*w/v*)	Crystallization Temperature (^{0}C)	Crystallization Time (Hour)	Yield (%)		Iodine Value (g I_2/100 g)	
				UCF	NUCF	UCF	NUCF
1	1 : 1.5	18	5	88.86	0.12	39.6	112.21
2	1 : 2	20	4	79.71	6.13	35.84	111.45
3	1 : 2	16.64	4	78.61	4.72	36.63	112.42
4	1 : 1.16	20	4	72.01	0.12	49.06	112.16
5	1 : 2	20	4	67.51	10.38	33.87	113.08
6	1 : 2	20	4	79.92	10.31	34.44	113.84
7	1 : 2	20	4	78.79	10.40	33.65	113.22
8	1 : 2.5	18	5	78.76	8.09	23.05	110.63
9	1 : 1,5	22	5	76.56	0.12	38.94	113.67
10	1 : 2	23.36	4	74.31	10.30	34.55	115.02
11	1 : 1.5	22	3	75.46	0.12	48.32	112.12
12	1 : 2.5	18	3	58.33	26.10	22.84	113.25
13	1 : 2.84	20	4	52.62	30.77	18.75	112.43
14	1 : 2.5	22	5	75.19	21.94	22.49	113.89
15	1 : 2.5	22	3	75.93	26.59	22.69	114.39
16	1 : 2	20	4	79.63	10.12	36.15	113.68
17	1 : 1.5	18	3	76.12	0.12	48.3	114.41
18	1 : 2	20	5.68	78.58	8.52	33.91	114.59
19	1 : 2	20	4	79.06	7.25	31.58	113.49
20	1 : 2	20	2.32	73.62	13.79	33.62	115.79

Table 3. Statistical model summary.

	Response			
	Yield UCF	**Yield NUCF**	**IV UCF**	**IV NUCF**
Model	Quadratic	Quadratic	Quadratic	Quadratic
Sum of Squares	943.38	1611.59	1406.40	24.87
Degree of freedom	9	9	9	9
Mean Square	104.82	179.07	156.27	2.76
F-Value	4.40	33.04	34.33	4,72
p-Value prob>F	0.0151	< 0.0001	< 0.0001	0.0118
Standard Deviation	4.88	2.33	2.13	0.76
R^2	0.7983	0.9675	0.97	0.81
Adjusted R^2	0.6168	0.9382	0.94	0.64
Predicted R^2	0.0761	0.7987	0.82	0.28
Press	1091.76	335.28	253.76	22.91

supported by its large model coefficient. Three-dimensional response surface plots demonstrated the interaction effects. The highest UCF yield (88.08%) was achieved at a ratio of 1:1.55, 18.16°C, and 5 h crystallization. The enhanced yield is attributed to efficient formation of urea-fatty acid inclusion complexes under these conditions.

$$Y_1 = 77.3 - 4.5A - 0.45B + 3.07C + 3.37AB + 0.73AC - 4.1BC - 4.42A^2 + 0.58B^2 + 0.45C^2 \quad (5)$$

Where Y_1 represents the yield of the UCF in percentage, A is the urea-to-methanol ratio expressed in weight per volume (w/v), B denotes the crystallization temperature in degrees Celsius (℃), and C refers to the crystallization time in hours (hrs).

Minimal deviation and random scattering of data points around the reference line indicate low random error and good model fitness, as shown in Figure 1 comparing predicted versus actual %yield of UCF.

The influence of the urea–methanol ratio and crystallization temperature on the predicted UCF yield is visualized through the response surface plots in Figure 2, with each subfigure representing a different crystallization time: 3 h, 4 h, and 5 h. Color gradients indicate variations in predicted yield, where blue represents the lowest and red the highest values.

As seen in the plots, a higher UCF yield is achieved at longer crystallization times, with the maximum predicted yield of 88.08% observed at 5 hours under a urea–methanol ratio of 1:1.55 and a crystallization temperature of 18.16°C. These optimal conditions are located in the red zone of the response surface, which also corresponds to high desirability values in the optimization function.

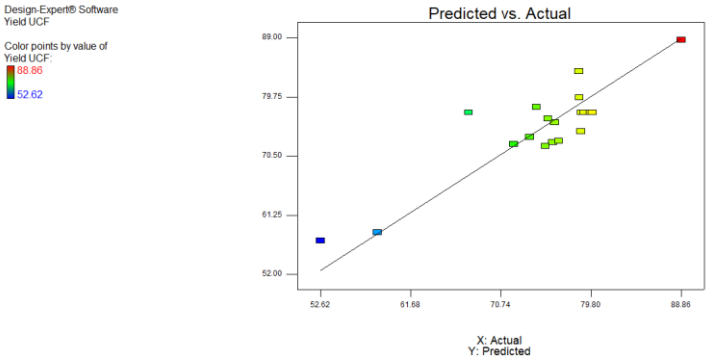

Figure 1. Graph of the relationship between actual and predicted results in the %Yield UCF model.

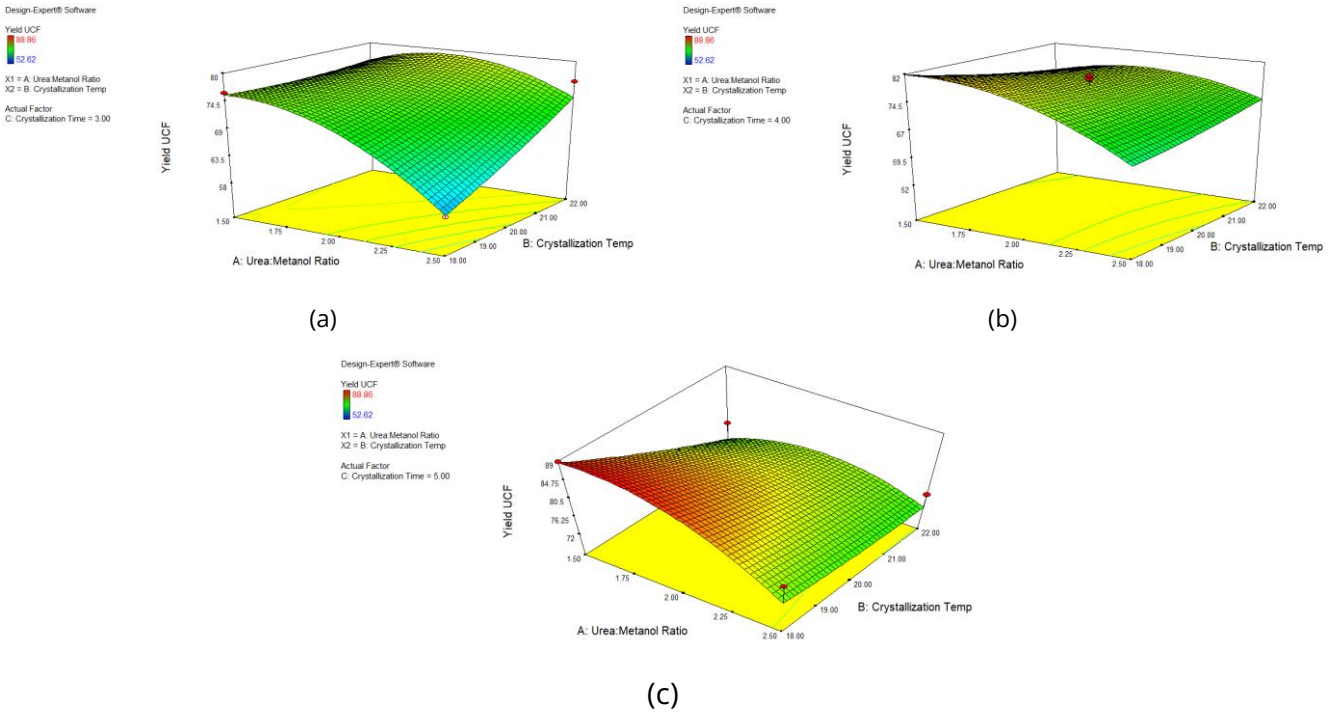

Figure 2. Three-dimensional response graph of %Yield UCF Interaction between urea-methanol ratio and crystallization temperature at crystallization times of 3 hours (b) 4 hours (c) 5 hours.

Among the three variables, crystallization time exhibited a lower individual significance based on the p-value; however, its effect became more apparent when combined with the other two variables, especially in the third plot. Therefore, 5 hours was identified as the optimal crystallization time for maximizing UCF yield under the studied conditions.

3.4. Effect of Process Variables on NUCF Yield

The normality test curve shows that the model meets the statistical assumptions. RSM analysis identifies the relationship between process variables and responses through coefficients in both coded and actual variable forms. The coded equation is used to indicate the relative influence of each variable on the yield and is presented in Equation 6.

$$Y_2 = 9.3 + 9.8A + 1.74B - 2.31C + 1.79AB - 2.83AC + 1.67BC + 2.01A^2 - 0.8B^2 + 0.49C^2 \quad (6)$$

Where Y_2 represents the yield of the NUCF in percentage, A is the urea-to-methanol ratio expressed in weight per volume (w/v), B denotes the crystallization temperature in degrees Celsius (℃), and C refers to the crystallization time in hours (hrs).

The accuracy of the model in predicting NUCF yield is demonstrated by the close alignment of data points along the diagonal reference line, as seen in the plot (Figure 3). This strong correlation between predicted and actual values indicates that the response surface model provides a reliable estimation with minimal systematic deviation. The residuals appear randomly distributed,

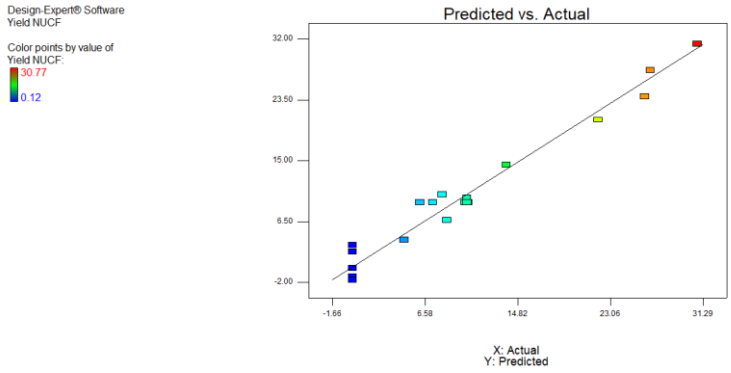

Figure 3. Graph of the relationship between actual and predicted results in the %Yield NUCF model.

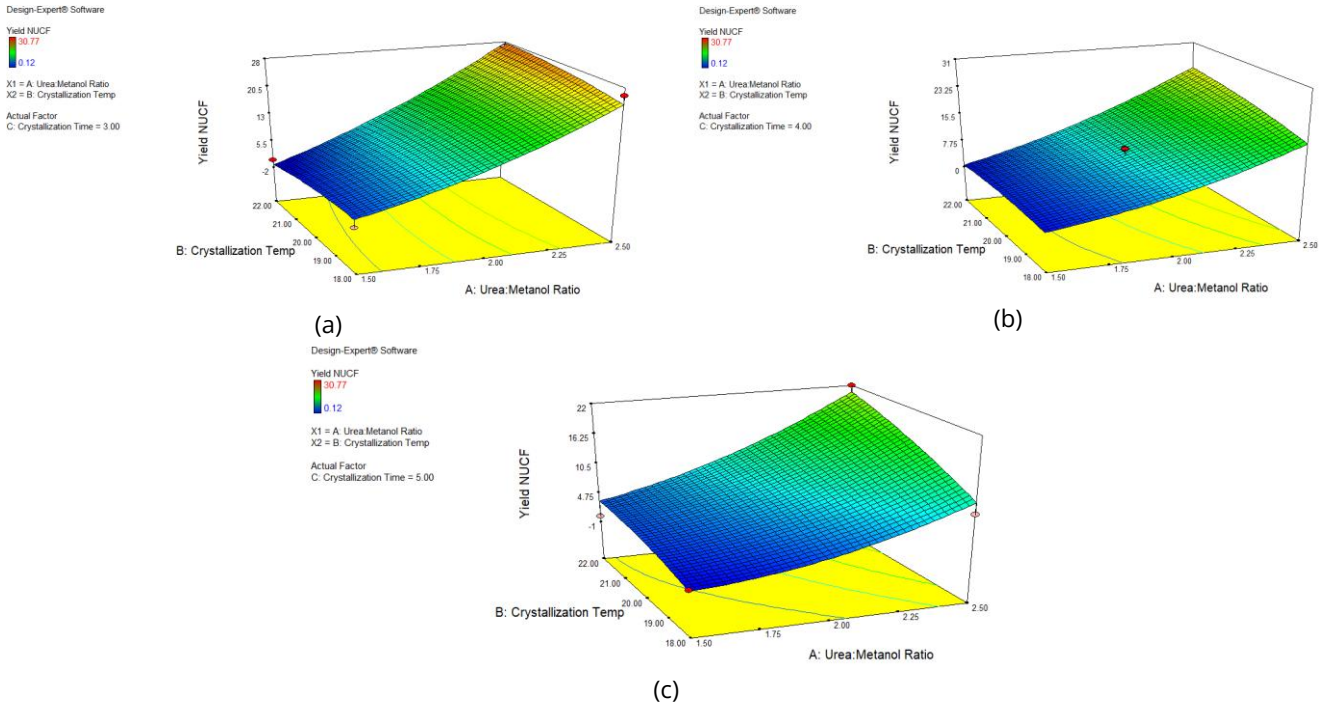

Figure 4. Three-dimensional response graph of %Yield NUCF interaction between urea-methanol ratio and crystallization temperature at crystallization times of 3 hours (b) 4 hours (c) 5 hours.

suggesting the absence of significant bias or non-linearity in the model.

Color-coded points, from blue (low yield) to red (high yield), also confirm that the model performs consistently across the entire experimental range. These results support the adequacy of the developed model for use in process optimization and confirm that the selected variables significantly influence the NUCF yield.

The combined effect of the urea–methanol ratio and crystallization temperature on the predicted NUCF yield is depicted in the response surface plots (Figure 4), with crystallization times fixed at 3, 4, and 5 hours respectively. A decreasing trend in NUCF yield is observed as the crystallization time increases, indicating a favorable condition for reducing the undesired fraction.

The lowest predicted NUCF yield of 1.76% was achieved at a crystallization time of 5 hours, using a urea–methanol ratio of 1:1.51 and a crystallization temperature of 19.31°C. These conditions are considered optimal for minimizing the formation of NUCF, which is advantageous in producing a biodiesel fraction enriched in saturated and monounsaturated FAMEs. While values as low as 0.12% were recorded, these were confirmed by repetition and align with prior reports, suggesting near-complete separation under optimized conditions.

3.5. Effect of Process Variables on Iodine Value of UCF

The equation in terms of coded variables for predicting the iodine value (IV) of the UCF fraction is shown in Equation 7.

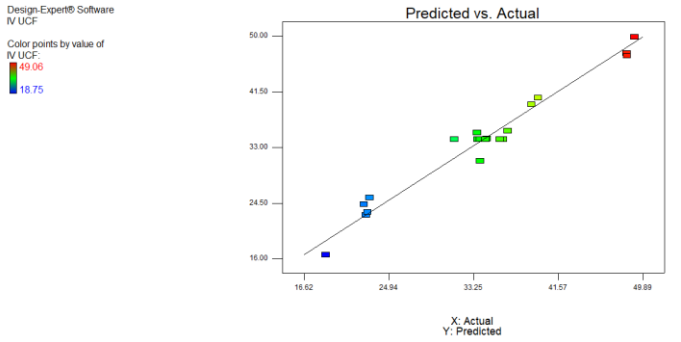

Figure 5. Graph of the relationship between actual and predicted results in the IV UCF model.

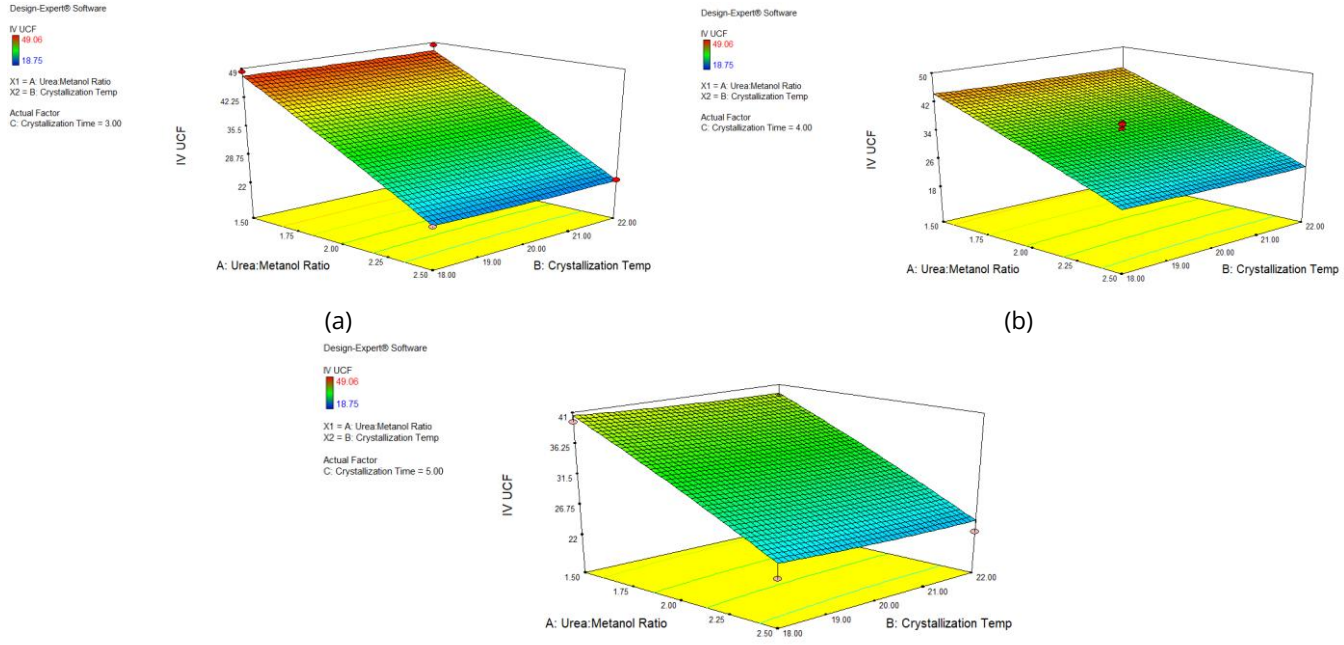

Figure 6. Three-dimensional response graph of IV UCF interaction between urea-methanol ratio and crystallization temperature at crystallization times of 3 hours (b) 4 hours (c) 5 hours.

$$Y_3 = 34.26 - 9.89A - 0.35B - 1.29C - 0.00875AB + 2.26AC - 0.14BC - 0.36A^2 + 0.24B^2 - 0.40C^2 \quad (7)$$

Where Y_3 represents the IV UCF (g I_2/100 g), A is the urea-to-methanol ratio expressed in weight per volume (w/v), B denotes the crystallization temperature in degrees Celsius (℃), and C refers to the crystallization time in hours (hrs).

The regression model indicates that all process variables have an influence on the iodine value of UCF. Among them, the urea-to-methanol ratio (A) has the most significant impact, as evidenced by its larger coefficient value compared to those of crystallization temperature (B) and crystallization time (C).

The predictive capability of the developed model is illustrated in Figure 5, which plots actual values on the X-axis against predicted values on the Y-axis. The data points are distributed closely along the diagonal line, indicating a strong correlation and good agreement between the experimental and model-predicted values.

Also shown in Figure 6 is the three-dimensional interaction between the urea-to-methanol ratio (A) and crystallization temperature (B) on the predicted iodine value (IV) of UCF, evaluated at three crystallization times: 3, 4, and 5 hours.

At a crystallization time of 3 hours, the desired IV UCF range of 30–40 g I_2/100 g was achieved when the urea-to-methanol ratio ranged from 1:1.8 to 1:2.1 and the crystallization temperature was between 18.44°C and 20.64°C, resulting in predicted IV values of 30.38–39.89 g I_2/100 g.

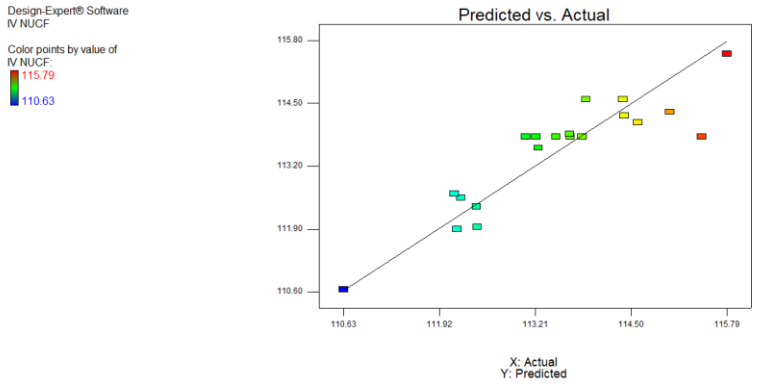

Figure 7. Graph of the relationship between actual and predicted results in the IV NUCF model.

Similarly, at 4 hours, the same IV UCF range was obtained with a urea-to-methanol ratio of 1:1.71 to 1:2.19 and crystallization temperatures from 19.93°C to 39.92°C, yielding predicted values between 30.51 and 39.44 g I_2/100 g.

At a crystallization time of 5 hours, the target IV range was also achieved within a urea-to-methanol ratio of 1:1.56 to 1:2.18 and a crystallization temperature range of 18.74°C to 20.15°C, with predicted values of 30.16–39.00 g I_2/100 g.

Based on these results, the optimum crystallization time is identified as 5 hours, with a urea-to-methanol ratio of 1:2.18 (w/v) and a crystallization temperature of 20.15°C.

3.6. Effect of Process Variables on Iodine Value of NUCF

The equation in terms of coded variables for predicting the iodine value (IV) of the NUCF fraction is expressed as shown in Equation 8.

$$Y_4 = 113.81 + 0.015A\ 0.58B - 0.42C - 0.65AB - -0.31AC + 0.73BC - 0.67A^2 - 0.17B^2 + 0.35C^2 \quad (8)$$

Where Y_3 represents the IV NUCF (g I_2/100 g), A is the urea-to-methanol ratio expressed in weight per volume (w/v), B denotes the crystallization temperature in degrees Celsius (℃), and C refers to the crystallization time in hours (hrs).

The model shows that all three process variables affect the iodine value of NUCF. Among them, the crystallization temperature (B) has the most pronounced positive effect, as indicated by the highest positive linear coefficient (+0.58), followed by crystallization time (C) with a negative influence (–0.42). The urea-to-methanol ratio (A), however, has only a minimal impact on the IV NUCF response based on its small linear coefficient (+0.015). Interaction and quadratic terms also contribute significantly, especially the BCBCBC interaction and A2A^2A2 term.

The model's predictive accuracy is shown in Figure 7, which presents a plot of actual versus predicted values for IV NUCF. The data points closely follow the diagonal line, indicating a good fit and high agreement between experimental results and model predictions.

The effect of the interaction between the urea-to-methanol ratio and crystallization temperature on the iodine value (IV) of NUCF at crystallization times of 3, 4, and 5 hours is illustrated in Figure 8. An increasing trend in IV NUCF was observed with longer crystallization times, particularly at specific combinations of urea-to-methanol ratios and temperatures. The maximum predicted IV of 114.85 g I_2/100 g was achieved at a crystallization time of 5 hours, using a ratio of 1:2.32 (w/v) and a temperature of 22.00°C. These results suggest that prolonged crystallization allows better exclusion of saturated FAME into urea complexes, thereby enriching NUCF with unsaturated fatty acids, which contribute to higher iodine values. Therefore, a crystallization time of 5 hours is considered the optimal condition for enhancing the iodine value of the NUCF fraction in the biodiesel fractionation process.

3.7. Optimization Using Desirability Function

Desirability-based optimization (Tables 4 and 5) balanced competing objectives: maximizing UCF yield and IV UCF while minimizing NUCF yield. Equal weights were assigned to all goals to ensure unbiased optimization. The optimum condition (1:1.71, 19.84°C, 5 h) achieved 82.05% UCF yield with 36.85 g I2/100 g IV, supporting the feasibility of the method to generate biodiesel fractions with improved oxidative stability.

3.8. Comparison with Literature and Standards

Compared to earlier studies focusing on single-variable optimizations, this research provides a more holistic approach. The iodine value achieved (36.65 g I2/100 g) aligns with European biodiesel standards (EN 14214),

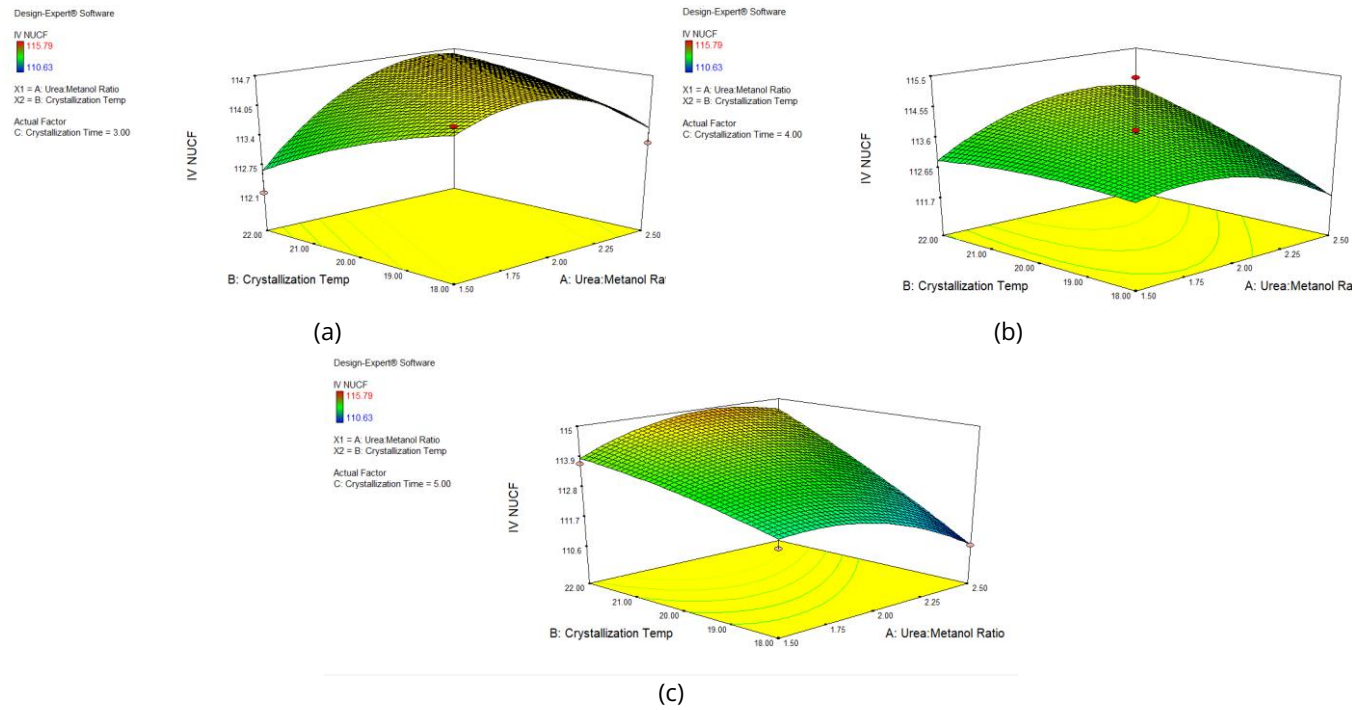

Figure 8. Three-dimensional response graph of IV NUCF interaction between urea-methanol ratio and crystallization temperature at crystallization times of 3 hours (b) 4 hours (c) 5 hours.

Table 4. Numerical optimization results of fractionation process conditions.

Description	Objective	Lower Limit	Upper Limit	Lower Weight Limit	Upper Weight Limit	Importance
Urea : Methanol Ratio	In range	1.5	2.5	1	1	3
Crystalization Temperature	In range	18	22	1	1	3
Crystalization Time	In range	3	5	1	1	3
Yield UCF	Maximize	52.62	88.86	1	1	3
Yield NUCF	Minimize	0.12	30.77	1	1	3
Iodine UCF	In range	30	40	1	1	3
Iodine NUCF	Maximize	110.63	115.79	1	1	3

Table 5. Optimization results of biodiesel fractionation process conditions.

No	Urea : Methanol Ratio	Crystalization Temperature	Crystalization Time	Yield UCF	Yield NUCF	IV UCF	IV NUCF	Desirability
1	1.73	19.99	5	81.59	4.09	36.65	113.7	0.75
2	1.73	19.94	5	81.75	4.12	36.53	113.69	0.75
3	1.71	19.84	5	82.05	3.8	36.85	113.62	0.75
4	1.7	19.82	5	82.07	3.64	37.08	113.6	0.75
5	1.71	19.72	5	82.44	3.62	36.92	113,56	0.75
6	1.76	20.05	5	81.43	4.49	36.16	113,76	0.75

which recommend lower unsaturation to reduce NOx emissions and oxidation.

3.9. Environmental and Practical Implications

Fractionating biodiesel into more saturated components improves oxidation stability, prolongs storage life, and reduces engine deposit formation. These improvements also reduce lifecycle GHG emissions due to enhanced combustion efficiency. Future work should validate these environmental claims via emissions testing and life cycle analysis.

3.10. Limitations and Future Research

This study was limited to FAME derived from palm-based biodiesel. Broader applicability across different feedstocks remains to be tested. Moreover, while compositional analysis confirms enrichment of SFA/MUFA in UCF, further structural characterization (e.g., GC-MS, FTIR) is recommended. Future research may

also explore real-engine testing and fuel blending behavior.

4. Conclusions

This study optimized the biodiesel fractionation process using the urea inclusion compound (UIC) method and response surface methodology (RSM) with a central composite design. The optimal conditions, urea: methanol ratio of 1:1.73, crystallization temperature of 19.99°C, and crystallization time of 5 hours, resulted in a high UCF yield of 81.59% and an iodine value (IV) of 36.65 g I_2/100 g. These values indicate that the UCF fraction is both quantitatively dominant and chemically saturated, making it suitable for producing biodiesel with improved oxidative stability and combustion performance. Additionally, this IV falls within the range required by international biodiesel standards (e.g., EN 14214).

The optimization process also successfully minimized the NUCF yield to as low as 1.76% under slightly different conditions, with an associated IV above 90 g I_2/100 g. This indicates the effective separation of unsaturated components into the NUCF fraction, further validating the robustness of the fractionation strategy.

While the model demonstrated strong predictive performance for UCF yield and IV UCF, some limitations were observed for IV NUCF, with an R^2 value of only 0.64. This suggests that further refinement is needed in modeling highly unsaturated components, possibly due to complex interactions or measurement variability. Additionally, the optimization focused on laboratory-scale conditions, and future work should address the scale-up feasibility and the influence of raw material variability.

The novelty of this study lies in its dual-objective optimization to maximize UCF quality and yield while minimizing NUCF, guided by statistical modeling. Compared to existing literature, few studies have systematically integrated desirability-based multi-response optimization in biodiesel fractionation using UIC. These findings not only advance the understanding of the crystallization mechanism in selective FAME inclusion but also provide a practical framework for producing high-performance biodiesel fractions.

From an environmental perspective, producing a more saturated biodiesel fraction offers advantages such as enhanced fuel shelf-life, lower emissions of particulate matter, and improved combustion efficiency. Future studies are recommended to validate these environmental benefits through empirical emissions testing, oxidative stability analysis, and life cycle assessment (LCA) to quantify the sustainability impact of optimized biodiesel.

Author Contributions: Conceptualization, Z.Z. and Z.H.; methodology, Z.Z. and Z.H.; software, Z.Z. and S.S.; validation, Z.H. and S.S.; formal analysis, Z.Z.; investigation, Z.Z.; resources, S.S.; data curation, Z.H.; writing—original draft preparation, Z.Z.; writing—review and editing, Z.H. and S.S.; visualization, Z.Z.; supervision, Z.H. and S.S.; project administration, Z.H.; funding acquisition, Z.H. All authors have read and agreed to the published version of the manuscript.

Funding: This study does not receive external funding.

Ethical Clearance: Not applicable.

Informed Consent Statement: Not applicable.

Data Availability Statement: The data that support the findings of this study are available from the corresponding author upon reasonable request.

Conflicts of Interest: All the authors declare no conflicts of interest.

References

1. Helwani, Z., Amraini, S. Z., Abd Rahman, S., Zahrina, I., Julhijah, N., and Ulfaa, S. M. (2024). Environmental Benefits of Palm Oil Biodiesel Enhancement: Urea Complexation Optimization via RSM, *Leuser Journal of Environmental Studies*, Vol. 2, No. 2, 62–74. doi:10.60084/ljes.v2i2.214.
2. Nur Aishah Rajali, Salina Mat Radzi, Maryam Mohamed Rehan, and Nur Amalina Mohd Amin. (2022). Optimization of the Biodiesel Production via Transesterification Reaction of Palm Oil Using Response Surface Methodology (RSM): A Review, *Malaysian Journal of Science Health & Technology*, Vol. 8, No. 2, 58–67. doi:10.33102/mjosht.v8i2.292.
3. Helwani, Z., Amraini, S. Z., Asmura, J., Siregar, T. N., Triwahyuni, V. E., and Abd, A. A. (2023). Palm Frond Waste as a Carbon Source in the Synthesis of CaO/Biochar Catalysts for the Biodiesel Production Process, *Heca Journal of Applied Sciences*, Vol. 1, No. 1, 8–13. doi:10.60084/hjas.v1i1.9.
4. Knothe, G. (2005). Dependence of Biodiesel Fuel Properties on the Structure of Fatty Acid Alkyl Esters, *Fuel Processing Technology*, Vol. 86, No. 10, 1059–1070. doi:10.1016/j.fuproc.2004.11.002.
5. Aydın, M., Uslu, S., and Bahattin Çelik, M. (2020). Performance and Emission Prediction of a Compression Ignition Engine Fueled with Biodiesel-Diesel Blends: A Combined Application of ANN and RSM Based Optimization, *Fuel*, Vol. 269, 117472. doi:10.1016/j.fuel.2020.117472.
6. Goto, S., Oguma, M., Chollacoop, N., Dowling, L., Sheedy, D., and Zhang, W. (2010). *EAS-ERIA Biodiesel Fuel Trade Handbook 2010*, ERIA, Jakarta.
7. Mofijur, M., Rasul, M. G., Hassan, N. M. S., Masjuki, H. H., Kalam, M. A., and Mahmudul, H. M. (2017). Assessment of Physical, Chemical, and Tribological Properties of Different Biodiesel Fuels, *Clean Energy for Sustainable Development*, Elsevier, 441–463. doi:10.1016/B978-0-12-805423-9.00014-4.
8. Bertoli, C., Fumeaux, R., Ferreira, M.-C. P., and Wang, J. (1997, October 21). Concentrate of Polyunsaturated Fatty Acid Ethyl Esters and Preparation Thereof, Google Patents.
9. Jiang, B., Liu, Y., Zhang, L., Sun, Y., Liu, Y., and Liu, X. (2014). Study on the Concentration of Unsaturated Fatty Acid Methyl Esters by Urea Complexation., *Journal of the Chemical Society of Pakistan*, Vol. 36, No. 6.

10. Guil-Guerrero, J. L., Rincón-Cervera, M. Á., and Venegas-Venegas, E. (2010). Gamma-linolenic and Stearidonic Acids: Purification and Upgrading of C18-PUFA Oils, *European Journal of Lipid Science and Technology*, Vol. 112, No. 10, 1068–1081. doi:10.1002/ejlt.200900294.

11. Hassan, N. M. (1994). The Adsorption of Long-Chain n-Paraffin from Isooctane Solution on Crystalline Urea, *Separations Technology*, Vol. 4, No. 1, 62–64. doi:10.1016/0956-9618(94)80007-3.

12. Bertoli, C., Fumeaux, R., Ferreira, M. C. P., and Wang, J. (1997). U.S. Patent No. 5,679,809, U.S. Patent and Trademark Office, Washington, DC.

13. Hayes, D. G., Bengtsson, Y. C., Van Alstine, J. M., and Setterwall, F. (1998). Urea Complexation for the Rapid, Ecologically Responsible Fractionation of Fatty Acids from Seed Oil, *Journal of the American Oil Chemists' Society*, Vol. 75, No. 10, 1403–1409. doi:10.1007/s11746-998-0190-9.

14. Guo, W., Zhu, Y., Han, Y., Luo, B., and Wei, Y. (2017). Separation Mechanism of Fatty Acids from Waste Cooking Oil and Its Flotation Performance in Iron Ore Desiliconization, *Minerals*, Vol. 7, No. 12, 244. doi:10.3390/min7120244.

15. Helwani, Z., Zahrina, I., Yelmida, Neonufa, G., Syamsuddin, Y., Rahmasari, A., Othman, M. R., and Idroes, R. (2023). Production of High-Performance Biodiesel with a High Oxidation Stability through a Fractionation Method Using Urea, *South African Journal of Chemical Engineering*, Vol. 45, 162–171. doi:10.1016/j.sajce.2023.05.009.

16. Baş, D., and Boyacı, İ. H. (2007). Modeling and Optimization I: Usability of Response Surface Methodology, *Journal of Food Engineering*, Vol. 78, No. 3, 836–845. doi:10.1016/j.jfoodeng.2005.11.024.

17. Shahidi, F., and Wanasundara, U. N. (1998). Omega-3 Fatty Acid Concentrates: Nutritional Aspects and Production Technologies, *Trends in Food Science & Technology*, Vol. 9, No. 6, 230–240. doi:10.1016/S0924-2244(98)00044-2.